Physics and Chemistry of Minerals
https://doi.org/10.1007/s00269-018-1015-5

Revision_1

H-bonding in lazulite: A single-crystal neutron diffraction study at 298 and 3 K

G. Diego Gatta, Pietro Vignola, Nicola Rotiroti and Martin Meven

Running title: Neutron diffraction study of lazulite

Corresponding author: G. Diego GATTA
Dipartimento di Scienze della Terra, Università degli Studi di Milano
Via Botticelli 23, I-20133 Milano, Italy
Tel. +39 02 503 15607, Fax +39 02 503 15597, E-Mail: diego.gatta@unimi.it

Manuscript submitted to Physics and Chemistry of Minerals

H-bonding in lazulite: A single-crystal neutron diffraction study at 298 and 3 K

G. Diego Gatta[1,2], Pietro Vignola[3], Nicola Rotiroti[1] and Martin Meven[4]

[1]Dipartimento di Scienze della Terra, Università degli Studi di Milano,
Via Botticelli 23, I-20133 Milano, Italy
[2] CNR-Istituto di Cristallografia, Via Amendola 122/O, I-70126 Bari, Italy
[3]CNR-Istituto per la Dinamica dei Processi Ambientali, via Botticelli 23, I-20133, Milano, Italy
[4]Institute of Crystallography, RWTH Aachen University, and Jülich Centre for Neutron Science (JCNS) at Heinz Maier-Leibnitz Zentrum (MLZ), Lichtenbergstraße 1, D-85747 Garching, Germany

Abstract

The crystal structure and crystal chemistry of a lazulite from Crosscut Creek (Kulan Camp area, Dawson mining district, Yukon, Canada) was investigated by electron microprobe analysis in wavelength-dispersive mode (EMPA) and single-crystal neutron diffraction at 298 and 3 K. Its empirical formula, based on EMPA data, is: $(Mg_{0.871}Fe_{0.127})_{\Sigma 0.998}Al_{2.030}(P_{1.985}Ti_{0.008}Si_{0.007}O_4)_2(OH)_2$. The neutron diffraction experiments at room and low *T* proved that the H-free structural model of lazulite previously reported, on the basis of X-ray structure refinement, is correct: the building unit of the lazulite structure consists of a group of three face-sharing (Al-octahedron)+(Mg,Fe-octahedron)+(Al-octahedron), connected to the adjacent one *via* a corner-shared OH-group and two corner-shared oxygen sites of the P-tetrahedron, to form a dense 3D-edifice. Only one crystallographically independent H site occurs in the structure of lazulite, forming a hydroxyl group with the O5 oxygen, with O5-H= 0.9997 Å at room temperature (corrected for *riding motion effect*). The H-bonding scheme in the structure of lazulite is now well defined: a bifurcated bonding scheme occurs with the O4 and O2 oxygen sites as *acceptors*. The two H-bonds are energetically different, as shown by their bonding geometry: the H-bond with the O2 site as *acceptor* is energetically more favorable, being O5-H···O2 = 152.67(9)°, O5···O2 = 3.014(1) Å and H···O2 = 2.114(1) Å, whereas that with O4 as *acceptor* is energetically more costly, being O5-H···O4 = 135.73(8)°, O5···O4 = 3.156(1) Å and H···O4 = 2.383(1) Å, at room temperature. No *T*-induced phase transition occurs within the *T*-range investigated. At low temperature, the O5-H···O2 bond is virtually identical to the room-*T* one, whereas the effects of *T* on O5-H···O4 are more pronounced, with significant differences of the $O_{donor}\cdots O_{acceptor}$ and $H\cdots O_{acceptor}$ distances. The experimental findings of this study do not support the occurrence of HPO_4 or H_2PO_4 units into the structure of lazulite, recently reported on the basis of infrared and Raman spectra.

Keywords: Lazulite; phosphates; single-crystal neutron diffraction; crystal chemistry; hydrogen bonding.

Introduction

Lazulite, $MgAl_2(PO_4)_2(OH)_2$, was described for the first time in the phosphate-bearing meta-quarzites at Freissnitzgraen (Krieglach, Styria, Austria) by Klaproth (1795). This phosphate belongs to the "lazulite group" and forms a series with its Fe-analogue scorzalite, $FeAl_2(PO_4)_2(OH)_2$ (Pecora and Fahey 1950). Lazulite occurs in metamorphic quartzites (phosphate-bearing quartzites), granitic pegmatites and low temperature hydrothermal veins in sedimentary or anchimetamorphic terranes.

Its crystal structure was solved in the $P2_1/c$ space group, with unit-cell parameters $a \sim 7.16$Å, $b \sim 7.26$ Å, $c \sim 7.24$ Å, $\beta \sim 120.7°$, by Lindberg and Christ (1959), using a specimen from Minas Gerais, Brazil. The anisotropic structural model was later refined by Giuseppetti and Tadini (1983) in the same space group, using a specimen from the Graves Mountains (Georgia, U.S.A.). Giuseppetti and Tadini (1983) provided also the potential coordinates of one independent H site (forming a hydroxyl group with O-H distances of about 0.8 Å). The structure models of Lindberg and Christ (1959) and Giuseppetti and Tadini (1983) are mutually consistent and show that the triple-groups of face-sharing (Al-octahedron)+(Mg,Fe-octahedron)+(Al-octahedron) are connected to the adjacent ones by a corner-shared OH-group and two corner-shared oxygen sites of the P-tetrahedron (Fig. 1). However, in a more recent paper, based on infrared and Raman investigations of lazulite, Frost et al. (2013) reported evidence of bending modes ascribed to tetrahedral PO_4, HPO_4 and H_2PO_4 units. These experimental findings are not consistent with the structural model reported by Lindberg and Christ (1959) and Giuseppetti and Tadini (1983), in which HPO_4 and H_2PO_4 groups are supposed not to occur. In addition, on the basis of their data, Frost et al. (2013) concluded that the proton on the hydroxyl units is apparently very mobile, promoting the formation of the monohydrogen and dihydrogen phosphate units.

In order to answer to the open questions about the structure of lazulite, and in the framework of a long-term project on the crystal-chemistry of hydrous phosphates (*e.g.*, Gatta et al. 2013a, 2013b, 2014a, 2014b, 2015; Rotiroti et al. 2016), we have reinvestigated the crystal chemistry of lazulite by electron microprobe analysis in wavelength-dispersive mode (EMPA) and single-crystal neutron diffraction, in order to provide: *i*) the reliable location of the proton site(s) and the real configuration of the OH-group(s), for a full description of the H-bonds; *ii*) the anisotropic displacement parameters of all the atomic sites, H-site(s) included. In order to reduce the thermal displacement of the H-sites, and to confirm or deny the assumption on the proton mobility reported by Frost et al. (2013), single-crystal neutron diffraction data were collected at room temperature (298 K) and at low temperature (3 K).

Sample description and occurrence

The crystal of lazulite used in this study belongs to the private collection of one of the authors (P.V., catalogue #1493) and comes from the Crosscut Creek (Kulan Camp area, Dawson mining district, Yukon, Canada). The crystal was taken from the surface of a druse (8 x 5 cm) representing a portion of the wall of a hydrothermally mineralized vein, with mineral association: lazulite + quartz + siderite. The phosphate rich clefts, in the Dawson mining district, are due to an unusual hydrothermal post-depositional history involving the whole Rapid Creek Formation (Robertson 1980, 1982). This complex sedimentary sequence, consisting of highly phosphatic ironstones, comprises (from the textural point of view) shales, mudstones, siltstones and sandstones. The phosphate mineral associations occur in the coarser layers as epigenetic fracture fillings in veins or vugs. Lazulite is part of a "complex vein", bearing a Ca-rich mineral association of the first type (*i.e.*, quartz + siderite + lazulite + "apatite"; Robertson 1982). This association typically takes place in veins perpendicular to the bedding of the mudstone host. The veins are about 40 cm wide and up to 10 m long.

Experimental methods

Quantitative EMPA in wavelength-dispersive mode was obtained from a polished and carbon-coated section using a JEOL JXA-8200 microprobe at the Earth Sciences Department, University of Milano (ESD-UMI). The system was operated using an accelerating voltage of 15 kV, a beam current of 5 nA, a beam diameter of 5 μm, and a counting time of 30 s on the peaks and 10 s on the backgrounds. The following standards were used: graftonite KF-16 for P, Fe, Mn, and Ca; grossular for Si and Al; K-feldspar for K; forsterite for Mg; omphacite for Na; ilmenite for Ti; realgar for As. Na, K, Ca, Mn and As were below the detection limits. The raw data were corrected for matrix effects using the protocol implemented in the JEOL suite of programs. The averaged composition of the lazulite used in this study is given in Table 1.

A single crystal of lazulite, optically homogeneous and free of inclusions or defects under a transmitted-light polarizing microscope, was selected for the X-ray and neutron diffraction experiments. A small fragment (0.31 x 0.27 x 0.17 mm^3) was first investigated by single-crystal X-ray diffraction. X-ray intensity data were collected at room temperature and up to $2\theta_{max} \cong 74°$ with a Xcalibur - Oxford Diffraction diffractometer at the ESD-UMI, equipped with a CCD, monochromatized Mo-*K*α radiation and operated at 50 kV and 30 mA. The X-ray data collection was performed with a combination of φ/ω scans, step size of 1° and an exposure time of 5 s/frame. The intensity data were integrated and indexed using the computer program CrysAlisPRO (Rigaku 2018). A total number of 8427 Bragg reflections, out of which 1062 were unique for symmetry

(Laue class: 2/*m*, R_{int} = 0.041), gave a metrically monoclinic unit-cell with: *a* = 7.139(1) Å, *b* = 7.288(1), *c* = 7.236(1), β = 120.33(2)°, according to the experimental findings of Giuseppetti and Tadini (1983), and the reflection conditions suggested the space group $P2_1/c$ as highly likely.

A larger fragment from the same crystal (2 x 2 x 3 mm) was then used for the monochromatic neutron diffraction experiments at room and low temperature, using the diffractometer HEiDi at the hot source (fast neutrons) of the neutron source FRM II of the Heinz Maier-Leibnitz-Zentrum (MLZ), Germany. The diffractometer was equipped with a ^{3}He single counter detector for high sensitivity down to short wavelengths. Two set of diffraction data were first collected at room temperature: a first set of data was collected with a wavelength of the incident beam of 1.171(1) Å (Ge-311 monochromator, Er foil to suppress λ/3 contamination) up to $2\theta_{max}$ = 121° (sin(θ)/λ = 0.74 Å^{-1}); a second set of data was collected at higher sin(θ)/λ up to 0.89 Å^{-1}, with a wavelength of the incident beam of 0.795(1) Å (Ge-422 monochromator, Er foil to suppress λ/2 contamination). In total, 2783 reflections were collected up to d_{min} ~ 0.7 Å (with – 12 ≤ *h* ≤ +12, -13 ≤ *k* ≤ +13 and -12 ≤ *l* ≤ +12, Table 2), using pure ω-scan and ω-2θ scan strategy as reported in Table 2, out of which 1755 were unique for symmetry and 1452 with F_o>4σ(F_o). Integrated intensities were then corrected for the Lorentz effect; absorption correction was found to be negligible. After the corrections, the discrepancy factor among symmetry-related reflections (Laue class: 2/*m*) was R_{int} = 0.0371 (Table 2).

Low-temperature diffraction data were collected with a wavelength of the incident beam of 0.795(1) Å. The sample was fixed on an aluminium pin (0.8 mm diameter) and mounted on a closed-cycle cryostat to reach a minimum temperature of 3.0 K (+/-0.1 K). A total number of 2047 reflections were collected up to d_{min} ~ 0.7 Å (with -11 ≤ *h* ≤ +11, -11 ≤ *k* ≤ +11 and -11 ≤ *l* ≤ +11, Table 2), using a pure ω-scan strategy, out of which 1292 were unique for symmetry and 986 with F_o>4σ(F_o). After corrected for the Lorentz effect, the discrepancy factor among symmetry-related reflections (Laue class: 2/*m*) was R_{int} = 0.0303 (Table 2). Further details pertaining to the neutron data collections, at room and low *T*, are given in Table 2.

For both the data collections (*i.e.*, room and low *T*), the lattice was found to be metrically monoclinic, and the reflections conditions were consistent with the space group $P2_1/c$, as previously reported by Giuseppetti and Tadini (1983). The evolution of intensity and full-width-at-half-maximum of three selected Bragg reflections (*i.e.*, 00-6, 040 and -400) were followed between room and low *T* (Fig. 2), showing no evidence of phase transition within the *T*-range investigated.

Anisotropic crystal-structure refinements, based on the neutron data collected at room and low *T*, were done in the space group $P2_1/c$ using the SHELXL-97 software (Sheldrick 1997, 2008), starting from the H-free structure model of Giuseppetti and Tadini (1983), and using the neutron

scattering lengths of Mg, Fe, Al, P, O and H from Sears (1986). Secondary isotropic extinction effect was corrected according to the formalism of Larson (1967), as implemented in the SHELXL package. After a few cycles of refinement, convergence was achieved with one (unique) intense negative residual peak in the final difference-Fourier map of the nuclear density (Fig. 3), located at *ca.* 1 Å from the O5 site. Further cycles of refinement were then done with H site assigned to this peak (as H has a negative neutron scattering length, Sears 1986). Convergence was achieved after a few cycles of refinement, with all the principal mean-square atomic displacement parameters positive, including those for the H site. At the end of the refinement, the variance-covariance matrix showed no significant correlation among the refined variables. Further details pertaining to structure refinement strategy are given in Table 2. Atomic coordinates and displacement parameters are listed in Tables 3 and 4; selected interatomic distances and angles are given in Table 5.

Results and Discussion

The EMPA data of the lazulite sample used in this study confirms its ideal formula: $MgAl_2(PO_4)_2(OH)_2$ (Pecora and Fahey 1950, Lindberg and Christ 1959). P (in tetrahedral coordination) is replaced by a very modest fraction of Ti and Si, Al (in octahedral configuration) does not show any substituent, and Mg is replaced by Fe (Table 1). The Mg *vs.* Fe substitution is expected, as lazulite (ideally $MgAl_2(PO_4)_2(OH)_2$) and scorzalite (ideally $FeAl_2(PO_4)_2(OH)_2$) are supposed to form a complete isomorphous series (Pecora and Fahey 1950; Gheith 1953). The empirical formula of lazulite from Crosscut Creek used in this study is: $(Mg_{0.871}Fe_{0.127})_{\Sigma 0.998}Al_{2.030}(P_{1.985}Ti_{0.008}Si_{0.007}O_4)_2(OH)_2$ (Table 1).

The neutron structure refinements of this study, based on intensity data collected at 298 and 3 K, provide a general structural model of lazulite consistent with those previously reported by Lindberg and Christ (1959) and Giuseppetti and Tadini (1983), based on single-crystal X-ray intensity data collected at room temperature: the building unit of the lazulite structure consists of a group of three face-sharing (Al-octahedron)+(Mg,Fe-octahedron)+(Al-octahedron), connected to the adjacent one *via* a corner-shared OH-group and two corner-shared oxygen sites of the P-tetrahedron, to form a dense 3D-edifice (Fig. 1). The P-tetrahedron is the most regular coordination polyhedron [with $\Delta(P\text{-}O)_{max} \sim 0.03$ Å, *i.e.*, the difference between the longest and the shortest bond distances], the (Mg,Fe)-octehedron is slightly more distorted [$\Delta(Mg,Fe\text{-}O)_{max} \sim 0.06$ Å], whereas the Al-octahedron is strongly deformed [$\Delta(Al\text{-}O)_{max} \sim 0.20$ Å]. Only one crystallographically independent H site occurs in the structure of lazulite, forming a hydroxyl group with the O5 oxygen, with O5-H*= 0.9997 Å at room temperature (*corrected for *riding motion effect*, Table 5). The H-

bonding scheme in the structure of lazulite is now well defined: a bifurcated bonding scheme occurs with the O4 and O2 oxygen sites as *acceptors* (Table 5). The two H-bonds are energetically different, as shown by their bonding geometry: the H-bond with the O2 site as *acceptor* is energetically more favorable, being O5-H···O2 = 152.67(9)°, O5···O2 = 3.014(1) Å and H···O2 = 2.114(1) Å, whereas that with O4 as *acceptor* is energetically more costly, being O5-H···O4 = 135.73(8)°, O5···O4 = 3.156(1) Å and H···O4 = 2.383(1) Å, at room temperature. At low temperature, the O5-H···O2 bond is virtually identical to the room-*T* one (differences are within 0.001 Å and 0.1°, Table 5), whereas the effects of *T* on O5-H···O4 are more pronounced, with significant differences of the O_{donor}···$O_{acceptor}$ and H···$O_{acceptor}$ distances (*i.e.*, ~0.02 Å, Table 5).

The H-bonding scheme in the structure of lazulite here described is compatible with the findings based on infrared and Raman spectroscopies (*e.g.*, Frost et al. 2013, RRUFF database: http://rruff.info/Lazulite), as IR and Raman spectra, in the region of the OH stretching active modes, show evidence of more than one unique H-bond. The description of the IR and Raman mode in lazulite provided by Frost et al. (2013) is likely affected by misinterpretation: the structure does not contain HPO_4 or H_2PO_4 units, and, in addition, the conclusion "*The proton on the hydroxyl units is apparently very mobile and enables the formation of the monohydrogen and dihydrogen phosphate units*" (Frost et al. 2013) is inconsistent with our experimental findings and, in general, not plausible. We expect that a more robust description of the active IR and Raman vibrational modes will be delivered on the basis of the structure models of this study.

As shown by the root-mean-square components of the displacement ellipsoids at room *T* (Table 4), the H site has the largest anisotropic displacement parameters, followed by the oxygen sites and then by the cationic sites. However, the disordered (Mg,Fe) site shows the largest displacement parameters among the cationic sites (*i.e.*, Mg-Fe, Al and P, Table 4). At low *T*, there is a general reduction of magnitude of the atomic displacement ellipsoids (by 10-40%), but not of their ellipticity ratio (Fig. 4, Table 4).

The Mg *vs.* Fe distribution is supposed not to change (at a significant level) between room and low *T*, as the mechanisms that promote intra-crystalline disordering, in this class of materials, are usually activated at high *T*. The slight difference between the refined Mg *vs.* Fe fraction at the octahedral site at room and low *T* are within 3σ (Table 3), and therefore not significant. On the average, we can assume that the chemical formula of lazulite based on the neutron structure refinements is $(Mg_{0.88(2)}Fe_{0.12(2)})Al_2(PO_4)_2(OH)_2$ (Table 3), in excellent agreement with the EMPA data.

Acknowledgements

The authors acknowledge the Heinz Maier-Leibnitz Zentrum (MLZ) in Garching, Germany, for the allocation of neutron beam time at the single-crystal diffractometer HEIDI, operated by RWTH Aachen University and Jülich Centre for Neutron Science, Forschungszentrum Jülich (JARA cooperation). GDG and NR acknowledge the support of the Italian Ministry of Education (MIUR) through the project "Dipartimenti di Eccellenza 2018-2022". E. Schingaro and an anonymous reviewer are thanked.

References

Busing WR, Levy HA (1964) The effect of thermal motion on the estimation of bond lengths from diffraction measurements. Acta Crystallogr 17:142-146.

Frost RL, Xi Y, Beganovic M, Belotti FM, Scholz R (2013) Vibrational spectroscopy of the phosphate mineral lazulite – $(Mg,Fe)Al_2(PO_4)_2(OH)_2$ found in the Minas Gerais, Brazil. Spectrochim Acta Part A (Molecular and Biomolecular Spectroscopy) 107:241-247.

Gatta GD, Vignola P, Meven M, Rinaldi R (2013a) Neutron diffraction in gemology: Single-crystal diffraction study of brazilianite, $NaAl_3(PO_4)_2(OH)_4$. Am Mineral 98:1624–1630.

Gatta GD, Nénert G, Vignola P (2013b) Coexisting hydroxyl groups and H_2O molecules in minerals: A single-crystal neutron diffraction study of eosphorite, $MnAlPO_4(OH)_2 \cdot H_2O$. Am Mineral 98:1297–1301.

Gatta GD, Jacobsen SD, Vignola P, McIntyre GJ, Guastella G, Abate LF (2014a) Single-crystal neutron diffraction and Raman spectroscopic study of hydroxylherderite, $CaBePO_4(OH,F)$. Mineral Mag, 78, 723-737.

Gatta GD, Vignola P, Meven M (2014b) On the complex H-bonding network in paravauxite, $Fe^{2+}Al_2(PO_4)_2(OH)_2 \cdot 8H_2O$: A single-crystal neutron diffraction study. Mineral Mag 78:841–850.

Gatta GD, Redhammer GJ, Vignola P, Meven M, McIntyre GJ (2015) Single-crystal neutron diffraction and Mössbauer spectroscopic study of hureaulite, $(Mn,Fe)_5(PO_4)_2(HPO_4)_2(H_2O)_4$. Eur J Mineral 28:93-103.

Gatta GD, Rotiroti N, Cámara F, Meven M (2018) On the labyrinthine world of arsenites: a single-crystal neutron and X-ray diffraction study of cafarsite. Phys Chem Minerals 45:819–829.

Gheith MA (1953) Lipscombite: a new synthetic "iron lazulite". Am Mineral 38:612-628.

Giuseppetti G, Tadini C (1983) Lazulite, $(Mg,Fe)Al_2(OH)_2(PO_4)_2$, structure refinement and hydrogen bonding. Neu Jb Mineral Mh. 1983:410-416.

Klaproth MH (1795) Beiträge zur chemischen Kenntnis der Mineralkörpe (first edition), Heinrich August Rottman, Berlin.

Larson AC (1967) Inclusion of secondary extinction in least-squares calculations. Acta Crystallogr 23:664 – 665.

Lindberg LM, Christ CL (1959) Crystal structures of the isostructural minerals lazulite, scorzalite and barbosalite. Acta Crystallogr 12:695-697.

Pecora WT, Fahey JJ (1950) The lazulite-scorzalite isomorphous series. Am Mineral 35:1-18.

Rigaku (2018) CrysAlisPRO, computer suite. Rigaku Oxford Diffraction.

Robertson BT (1980) Stratigraphic setting of some new and rare phosphate minerals in the Yukon Territory. M.Sc. Thesis, University of Saskatchewan, Saskatoon, Canada.

Robertson BT (1982) Occurrence of epigenetic phosphate minerals in a phosphatic iron-formation, Yukon Territory. Can Mineral 20:177-187.

Rotiroti N, Vignola P, Bersani D, Simmons WB, Falster AU, Whitmore RW, Nizamoff J, Lotti P, Risplendente A, Pavese A (2016) On the crystal-chemistry of bjarebyite, $BaMn^{2+}_2Al_2(PO_4)_3(OH)_3$, from the Palermo #1 pegmatite, Grafton County, New Hampshire, USA. Can Mineral 54:1033-1041.

Sears VF (1986) Neutron Scattering Lengths and Cross-Sections. In K. Sköld and D.L. Price, Eds., Neutron Scattering, Methods of Experimental Physics, Vol. 23A, 521-550. Academic Press, New York.

Sheldrick GM (1997) SHELXL-97. Programs for crystal structure determination and refinement. University of Göttingen, Germany.

Sheldrick GM (2008) A short history of SHELX. Acta Crystallogr A64:112-122.

Table 1. EMPA chemical analysis of lazulite from Crosscut Creek (Kulan Camp area, Dawson mining district, Yukon, Canada). Average composition based on 9 point-analysis.

	wt %	*e.s.d.*		**a.p.f.u.*
P_2O_5	45.61	0.20	P	1.985
SiO_2	0.13	0.05	Si	0.007
TiO_2	0.21	0.10	Ti	0.008
Al_2O_3	33.51	0.18	sum	**2.000**
FeO	2.96	0.18		
MgO	11.37	0.12	Al	**2.030**
H_2O**	5.83	0.03		
Total	99.63		Fe	0.127
			Mg	0.871
			sum	**0.998**
			H**	**2.000**

Notes: *calculated on the basis of 2 (P+Si+Ti) *a.p.f.u.*; ** calculated on the basis of 2 OH-groups.

Table 2. Details of neutron data collections and refinements of lazulite.

T (K)	298	3
Crystal shape	Prism	Prism
Crystal volume (mm)	2 x 2 x 3	2 x 2 x 3
Unit-cell parameters	a = 7.139(1) Å	a = 7.137(1) Å
	b = 7.288(1) Å	b = 7.249(1) Å
	c = 7.236(1) Å	c = 7.201(1) Å
	β = 120.33(2)°	β = 120.38(5)°
Reference chemical formula	$MgAl_2(PO_4)_2(OH)_2$	$MgAl_2(PO_4)_2(OH)_2$
Space Group	$P2_1/c$	$P2_1/c$
Z	2	2
Radiation type	neutron	neutron
Wavelength (Å)	1.171(1), 0.795(1)	0.795(1)
Diffractometer	HEiDi-4circle	HEiDi-4circle
Data-collection method	ω-scan, ω-2θ scan	ω-scan
d_{min} (Å)	~ 0.7	~ 0.7
	$-12 \le h \le +12$	$-11 \le h \le +11$
	$-13 \le k \le +13$	$-11 \le k \le +11$
	$-12 \le l \le +12$	$-11 \le l \le +11$
Measured reflections	2783	2047
Unique reflections	1755	1292
Unique reflections with $F_o > 4\sigma(F_o)$	1452	986
Refined parameters	82	81
R_{int}	0.0371	0.0303
R_σ	0.0381	0.0407
R_1 *(F)* with $F_o > 4\sigma(F_o)$	0.0328	0.0293
R_1 *(F)* for all reflections	0.0580	0.0528
$wR_2(F^2)$	0.0578	0.0454
GooF	1.627	1.291
Residuals (fm/Å^3)	-0.9/+0.8	-0.7/+0.6

Note: Statistical parameters according to the Shelxl-97 definition (Sheldrick 1997, 2008). Unit-cell parameters at room T based on single-crystal X-ray diffraction data. Further details pertaining to the data collection protocols are in Gatta et al. (2018).

Table 3. Refined fractional atomic coordinates and equivalent/isotropic displacement factors (Å^2), based on the neutron structure refinements of lazulite at 298 and 3 K. U_{eq} is defined as one-third of the trace of the orthogonalised U_{ij} tensor.

Site	*s.o.f.*	*x/a*	*y/b*	*z/c*	U_{eq}
298 K					
Mg	Mg 0.895(5), Fe 0.105(5)	0	0	0	0.00775(13)
Al	Al 1	-0.26734(8)	0.26678(8)	0.00630(10)	0.00574(10)
P	P 1	0.24810(6)	0.38541(5)	0.24507(7)	0.00544(8)
O1	O 1	-0.21236(6)	0.01394(5)	0.10605(7)	0.00877(8)
O2	O 1	-0.28791(6)	0.49997(5)	-0.09320(7)	0.00973(8)
O3	O 1	0.04396(5)	0.26401(5)	0.12474(6)	0.00873(8)
O4	O 1	-0.56186(5)	0.24243(6)	-0.12910(6)	0.00948(8)
O5	O 1	-0.26002(6)	0.14638(5)	-0.24144(6)	0.00735(8)
H	H 1	-0.38416(14)	0.06336(13)	-0.30098(15)	0.02493(18)
3 K					
Mg	Mg 0.876(7), Fe 0.124(7)	0	0	0	0.00288(17)
Al	Al 1	-0.26714(13)	0.26665(11)	0.00617(14)	0.00212(13)
P	P 1	0.24796(9)	0.38489(7)	0.24490(9)	0.00209(8)
O1	O 1	-0.21312(8)	0.01366(7)	0.10528(8)	0.00330(9)
O2	O 1	-0.28733(8)	0.50023(7)	-0.09256(8)	0.00351(9)
O3	O 1	0.04361(8)	0.26334(7)	0.12493(8)	0.00339(9)
O4	O 1	-0.56178(8)	0.24354(7)	-0.12952(8)	0.00351(9)
O5	O 1	-0.25998(9)	0.14669(7)	-0.24130(9)	0.00317(9)
H	H 1	-0.38447(18)	0.06335(16)	-0.30080(19)	0.0181(2)

Table 4. Refined displacement parameters (Å^2) in the expression: $-2\pi^2[(ha^*)^2U_{11} + \ldots + 2hka^*b^*U_{12} + \ldots + 2klb^*c^*U_{23}]$ and root-mean-square displacement amplitude (*RMS*, Å), based on the neutron structure refinements of lazulite at 298 and 3 K.

	U_{11}	U_{22}	U_{33}	U_{12}	U_{13}	U_{23}	*RMS-min*	*RMS-mid*	*RMS-max*	*max/min*
298 K										
Mg	0.0085(2)	0.0065(2)	0.0097(2)	0.0017(1)	0.0056(2)	0.0006(2)	0.0714	0.0888	0.1013	1.42
Al	0.0055(2)	0.0057(2)	0.0057(2)	0.0001(1)	0.0026(2)	0.0002(2)	0.0732	0.0753	0.0786	1.07
P	0.0054(1)	0.0051(1)	0.0057(1)	-0.0002(1)	0.0027(1)	-0.0001(1)	0.0709	0.0739	0.0764	1.08
O1	0.0115(1)	0.0075(1)	0.0098(2)	0.0017(1)	0.0072(1)	0.0024(1)	0.0752	0.0880	0.1138	1.51
O2	0.0149(2)	0.0068(1)	0.0108(2)	0.0008(1)	0.0090(1)	0.0018(1)	0.0734	0.0916	0.1241	1.69
O3	0.0058(1)	0.0082(1)	0.0104(2)	-0.0011(1)	0.0028(1)	-0.0024(1)	0.0722	0.0886	0.1145	1.58
O4	0.0061(1)	0.0101(1)	0.0107(2)	-0.0017(1)	0.0032(1)	-0.0028(1)	0.0737	0.0962	0.1173	1.59
O5	0.0083(1)	0.0074(1)	0.0061(1)	-0.0006(1)	0.0034(1)	0.0001(1)	0.0777	0.0842	0.0944	1.22
H	0.0250(3)	0.0285(4)	0.0202(4)	-0.0140(3)	0.0106(3)	-0.0057(3)	0.1122	0.1448	0.2031	1.81
3 K										
Mg	0.0037(3)	0.0024(3)	0.0030(3)	0.0006(2)	0.0020(2)	0.0001(2)	0.0446	0.0523	0.0625	1.40
Al	0.0030(3)	0.0018(3)	0.0020(3)	-0.0001(2)	0.0016(2)	0.0001(2)	0.0380	0.0438	0.0547	1.44
P	0.0025(2)	0.0018(2)	0.0021(2)	-0.0001(2)	0.0013(1)	-0.0003(2)	0.0390	0.0468	0.0505	1.29
O1	0.0047(2)	0.0027(2)	0.0035(2)	0.0002(2)	0.0029(2)	0.0011(2)	0.0374	0.0593	0.0704	1.88
O2	0.0055(2)	0.0023(2)	0.0038(2)	0.0001(2)	0.0033(2)	0.0007(2)	0.0413	0.0562	0.0751	1.82
O3	0.0031(2)	0.0029(2)	0.0038(2)	-0.0009(2)	0.0015(2)	-0.0008(1)	0.0449	0.0620	0.0657	1.46
O4	0.0030(2)	0.0036(2)	0.0037(2)	-0.0007(1)	0.0015(2)	-0.0010(1)	0.0490	0.0589	0.0683	1.39
O5	0.0042(2)	0.0031(2)	0.0027(2)	-0.0003(1)	0.0020(1)	0.0001(1)	0.0470	0.0552	0.0652	1.39
H	0.0179(4)	0.0192(5)	0.0164(4)	-0.0108(4)	0.0081(4)	-0.0043(3)	0.0880	0.1301	0.1719	1.95

Table 5. Relevant bond distances (Å) and angles (°) based on the neutron structure refinements at 298 and 3 K.

	298 K	*3 K*
Mg - O1 x 2	2.0181(5)	2.0161(6)
Mg - O3 x 2	2.0807(4)	2.0657(5)
Mg - O5 x 2	2.0882(6)	2.0813(6)
Al - O1	1.9454(7)	1.9347(10)
Al - O2	1.8224(7)	1.8137(10)
Al - O3	1.9366(7)	1.9319(10)
Al - O4	1.8253(8)	1.8239(10)
Al - O5	2.0200(8)	2.0066(11)
Al - O5'	1.9074(8)	1.9000(11)
P - O1	1.5429(5)	1.5389(8)
P - O2	1.5171(6)	1.5125(8)
P - O3	1.5438(6)	1.5412(7)
P - O4	1.5133(6)	1.5121(7)
O5 - H	0.9755(9)	0.9761(11)
O5 – H*	0.9997	0.9968
O5 - H···O2	152.67(9)	152.7(1)
O5···O2	3.014(1)	3.015(1)
H···O2	2.114(1)	2.113(1)
O5 - H···O4	135.73(8)	135.6(1)
O5···O4	3.156(1)	3.135(1)
H···O4	2.383(1)	2.362(1)

* Bond distance corrected for "riding motion" effect following Busing and Levy (1964)

Figure 1. The crystal structure of lazulite, viewed down [010] (*top left*) and [100] (*top right*), and its bifurcated H-bonding scheme (*bottom left*), based on the neutron structure refinement of this study (intensity data collected at 298 K). Displacement ellipsoid probability factor: 50%. In bracket: the triple face-sharing Al_{oct}-$(Mg,Fe)_{oct}$-Al_{oct} building unit (*bottom right*).

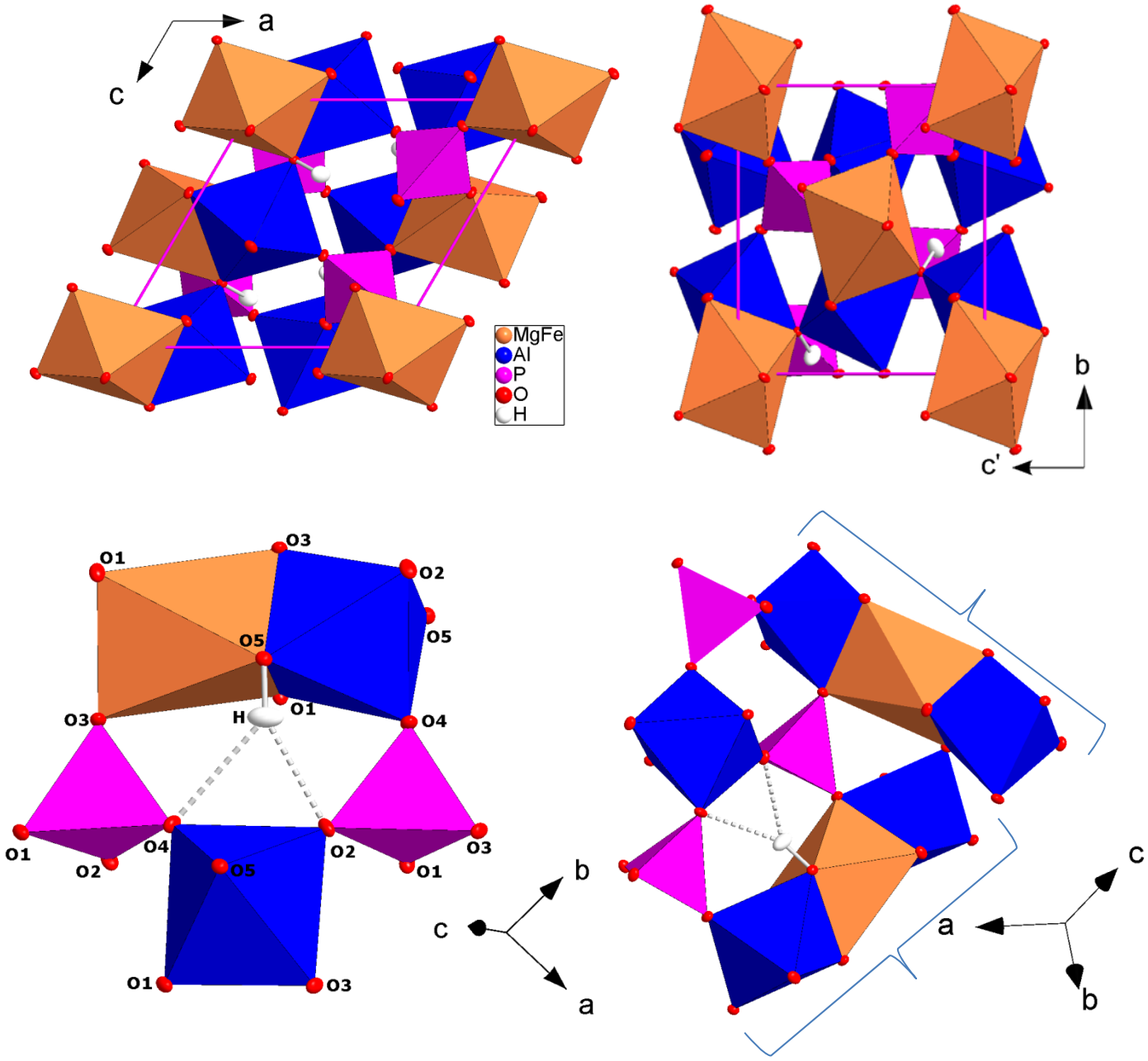

Figure 2. Evolution of the integrated intensities and of the full-width-at-half-maxima (FWHM) of the Bragg reflections 00-6 (*top left and right*), 040 (*mid left and right*) and -400 (*bottom left and right*) with *T*.

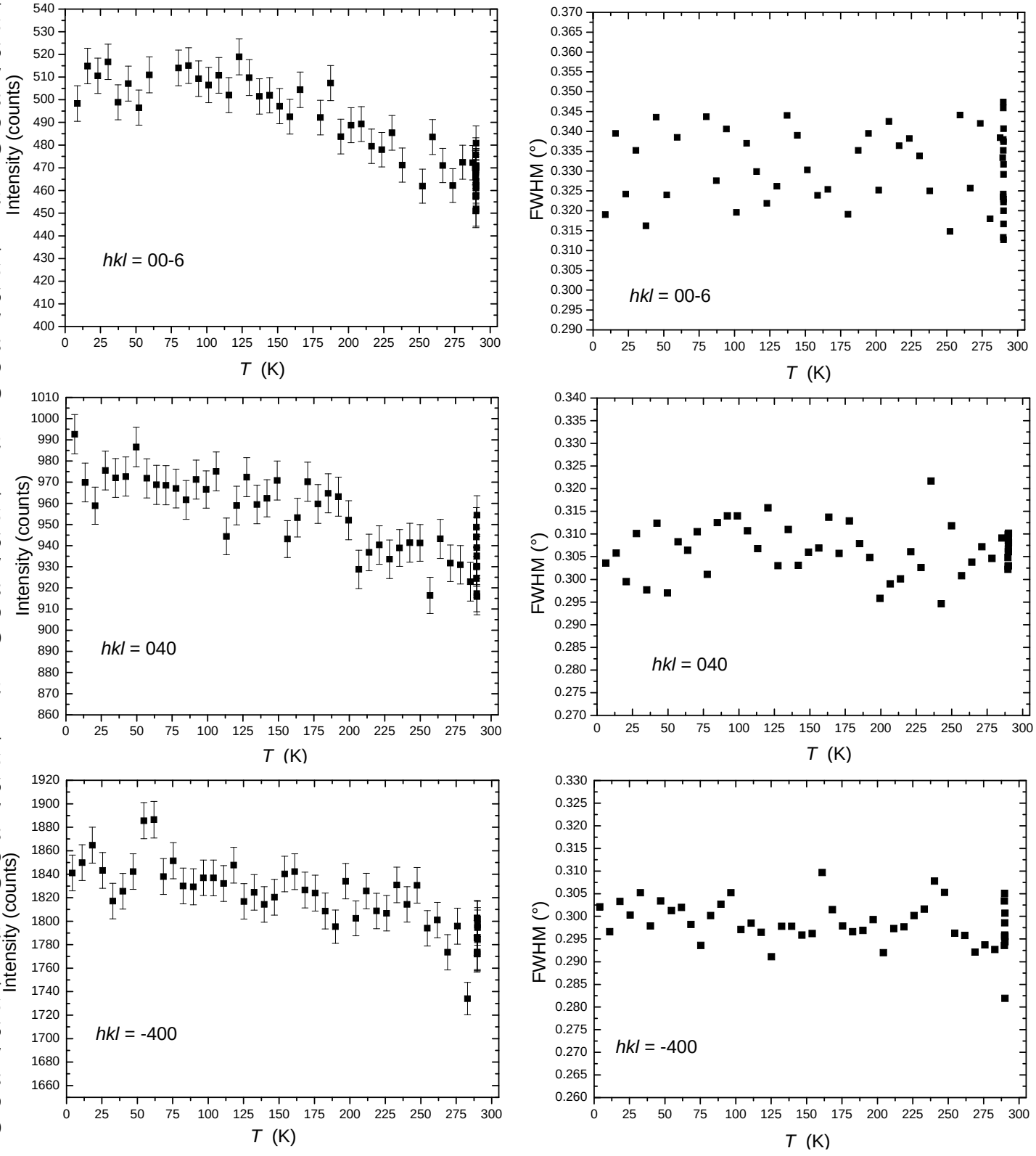

Figure 3. Difference-Fourier maps of the nuclear density (*xy* sections, *x* horizontal; $z \sim 0.7$) at 298 K (*top*) and at 3 K (*down*), calculated with coefficients *Fo-Fc* and phased by *Fc*. The *Fc* were calculated from a structural model without the H site. Color bar unit: fm/Å^3.

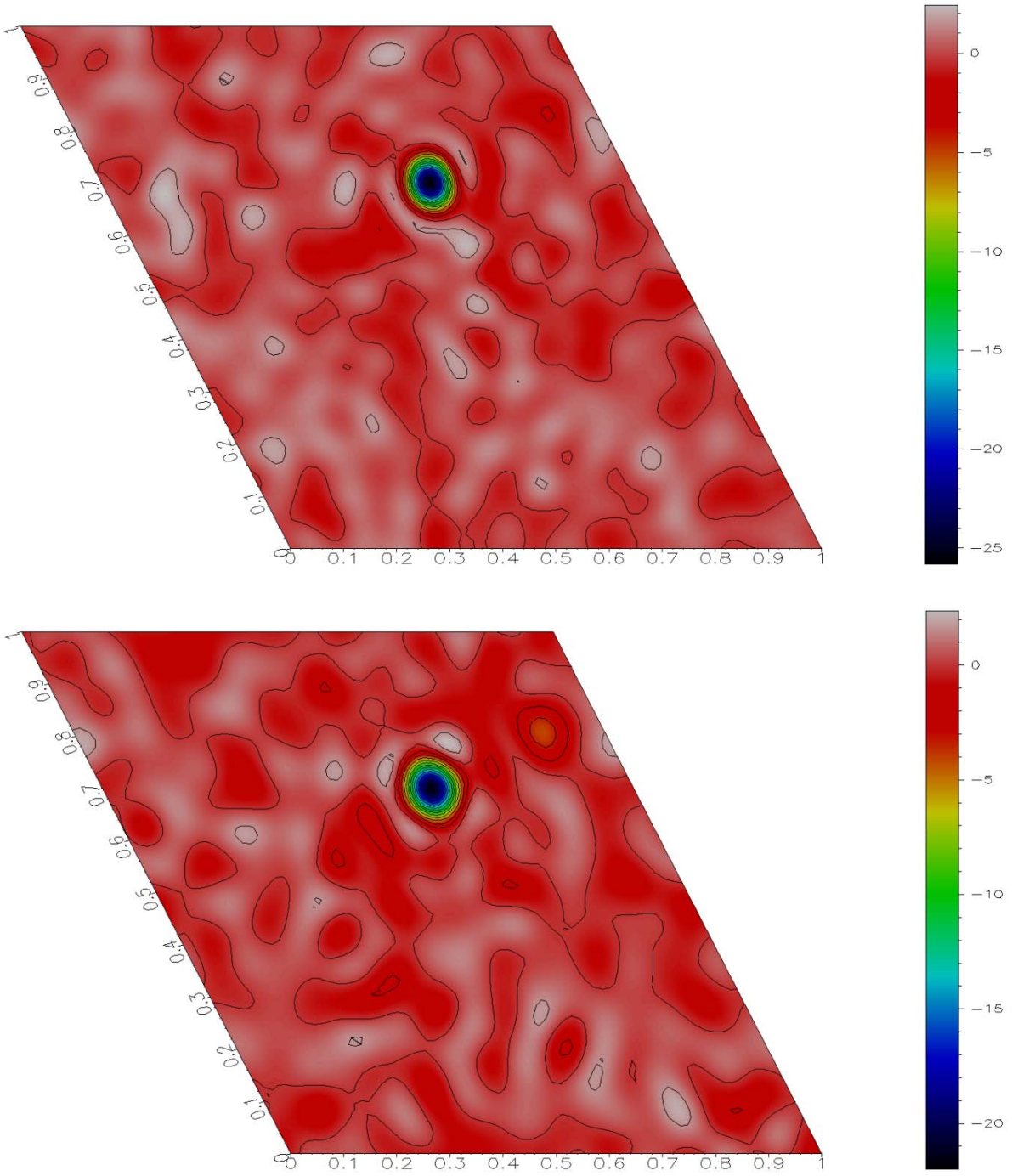

Figure 4. Magnitude of the atomic displacement ellipsoids, with probability factor 99%, based on the structure refinements at 298 K (*left side*) and at 3 K (*right side*). Colors and orientations as in Fig. 1.